An Investigation of Potential Impacts of Wind Turbines and Foundations on the Cold Pool

Authors and Affiliation:

Travis Miles, Ph.D. Associate Professor. Principal Investigator
tnmiles@marine.rutgers.edu

L. Fernando Pareja-Roman, Ph.D. Assistant Research Professor. Co-Investigator.
pareja@marine.rutgers.edu

Rutgers University - Department of Marine and Coastal Sciences
Center for Ocean Observing Leadership.

Prepared for:

New Jersey Department of Environmental Protection and
New Jersey Board of Public Utilities

Project Managers:
Caitlin McGarigal, NJDEP Division of Science and Research
Jesse Kolodin, NJBPU Division of Clean Energy

July, 2025

Department of Environmental Protection
Shawn M. LaTourette, Commissioner

State of New Jersey
Phil Murphy, Governor

Board of Public Utilities
Christine Guhl-Sadovy, President

Visit the Research and Monitoring Initiative website: https://dep.nj.gov/offshorewind/rmi/

Acknowledgements:

Funded by the New Jersey Department of Environmental Protection and the New Jersey Board of Public Utilities as a part of the New Jersey Offshore Wind Research and Monitoring Initiative through an agreement with Rutgers, The State University of New Jersey under Contract Number BC22-001-006.

Please cite as:

Miles, T.; Pareja-Roman, L.F. 2025. An Investigation of Potential Impacts of Wind Turbine and Foundations on the Cold Pool. New Jersey Department of Environmental Protection. Trenton, NJ. 32 pages, Available at https://hdl.handle.net/10929/148055

Table of Contents

Executive Summary

This project investigates how offshore wind farms (OWFs) may alter ocean mixing and stratification in the U.S. Mid-Atlantic Bight (MAB), with a specific focus on the Cold Pool—an ecologically critical bottom layer of cold water that forms in spring, persists through summer, and breaks down in fall. As OWF development is carried out along the U.S. East Coast, scientific understanding of how turbine foundations and wind wakes affect coastal oceanography remains limited. This study addresses high-priority questions outlined by the New Jersey Offshore Wind Research and Monitoring Initiative (RMI), particularly the potential impacts of OWFs on ocean stratification and circulation patterns. The project comprises two tasks:

Task 1 estimates the time scale required for turbine foundations to mix a stratified water column in the MAB. We apply an analytical model originally developed for the North Sea (Carpenter et al., 2016) and tailor it to MAB conditions. Monopiles are idealized as rigid cylinders generating turbulence when exposed to flow. Inputs include glider-based stratification, current speeds from a regional data-assimilative ocean model, and turbine diameters and spacing. Results show that under typical tidal velocities (~0.1 m/s), OWFs would require nearly 27 years to mix the Cold Pool. Even with strong storm-driven currents, mixing would require sustained flow well beyond what typically occurs on the MAB shelf. While OWFs are unlikely to de-stratify the Cold Pool, localized mixing and flow disturbances may still occur.

Task 2 evaluates how turbine-induced wind wakes affect surface momentum and heat fluxes. Using the Rutgers University Weather Research and Forecasting (RUWRF) model, we simulate atmospheric conditions with and without turbines under summertime conditions. Our results confirm that wind speed reductions at the ocean surface (~0.5 m/s) and friction velocity changes (~0.02 m/s) are expected to be minor and spatially confined to wind farm areas. Modeled surface temperature changes (±0.05°C) and associated sensible heat flux differences were also small. These findings align with those of Golbazi et al. (2022), who found minimal surface impacts from ‘extreme-scale’ turbines in the MAB, which they defined as turbine diameter and hub height greater than 150 and 100 m, respectively.

Together, these results suggest that OWFs will likely have limited capacity to fully mix the Cold Pool through either subsurface mixing or surface wake processes. However, the cumulative effects during seasonal transitions and under high-current events warrant continued study. This work informs both offshore wind development and coastal resource management in the MAB.

1. Introduction

1.1 Motivation

Offshore wind farm (OWF) development has been accelerating rapidly with the potential to contribute significantly to renewable energy production. However, the impact of turbine foundations and wind wakes on the underlying water column and ecosystems is not well observed or modeled. Understanding how these farms affect water mixing and density stratification in the water column proves critical for sustainable development and regional economic growth. Ocean currents interact with wind farm foundations—whether monopiles or tripods—to generate turbulence and flow separation. These interactions can scour sediments, redistribute nutrients, and reduce light penetration into the water column, potentially impacting marine ecosystems from phytoplankton to marine mammals. Research has not yet addressed these impacts in the Mid-Atlantic Bight (MAB), a region that supports sustainable offshore wind development and marine resource management.

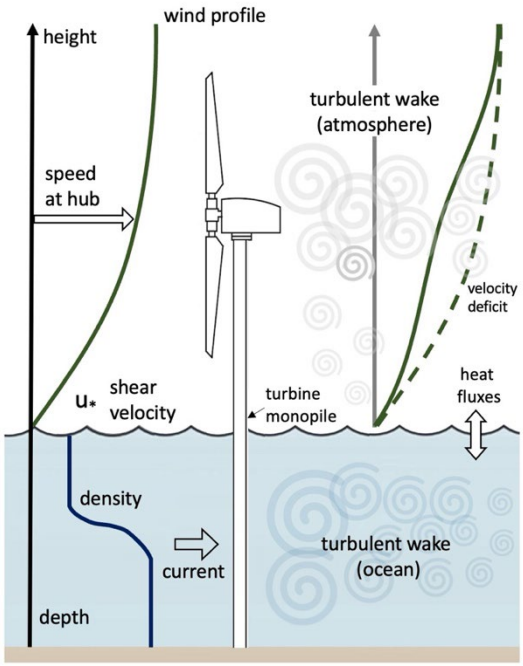

Figure 1. Schematic of Mixing in the Ocean and Atmosphere due to Wind Turbines.

The MAB extends from Cape Hatteras, North Carolina, to Cape Cod, Massachusetts, on the U.S. east coast. Local topography, freshwater discharge, seasonal stratification, and storm events drive its oceanography. In summer, the region develops a cold bottom layer known as the "Cold Pool," which is a unique regional oceanographic feature (Houghton et al., 1982; Lentz, 2017) that structures the physical water column and ecosystem (Miles et al., 2021). This feature is formed through rapid ocean warming due to atmospheric and solar heating in spring and summer (Lentz, 2017), which traps cold bottom winter water and isolating it from the sea surface. The Cold Pool is supported by additional cold water transported from the north allowing these cold temperatures and associated habitat to

persist through summer and into the fall. Ultimately the Cold Pool is broken down each year through storm driven ocean mixing and reduced seasonal heating with the transition from summer to fall. The Cold Pool modulates primary production (Falkowski et al., 1983; Flagg et al., 1994), as well as migratory fish (Secor et al., 2019) and shellfish ecology (Sower et al., 2022). The shellfish industry generates nearly 80% of the area's fishing revenue, so managers must understand Cold Pool dynamics to conserve resources and guide policy.

Studies in the North Sea, Europe (Carpenter et al., 2016), demonstrate that wind farm foundations can increase ocean mixing, which depends on monopile spacing, water depth, and most importantly, current speeds. The North Sea features semi-diurnal tidal currents of about 0.3-0.4 m/s and relatively weak stratification. In the MAB, semi-diurnal tides are in the order of 0.1 m/s, with episodic storm-driven currents exceeding 0.5 m/s. These differences, combined with variations in turbine design between regions, call for research tailored to the MAB.

Modeling the hydrodynamic effects of OWFs has unique challenges, requiring the representation of small-scale turbulence around individual turbines and larger wind farm-scale interactions spanning tens of kilometers (Figure 1). Researchers often rely on computational, observational, and analytical approaches to address these challenges. Atmospheric models such as Weather Research and Forecasting (WRF), used in this study, parameterize wind farms as sources of drag and energy sinks in the atmosphere (Fitch et al., 2012; Skamarock et al., 2019). In contrast, regional ocean models (Haidvogel et al., 2008) lack similar parameterizations for turbine foundation-induced mixing (Figure 1) in the ocean. Large Eddy Simulation models of the ocean can be used to study these interactions but typically focus on small resolutions (~ 1 m), localized domains (<1 km) and are computationally expensive.

In addition to mixing in the water column, wind turbines modify the structure of the marine atmospheric boundary layer by converting energy from the mean wind profile into usable electricity. This energy conversion creates a wind speed deficit and generates turbulent wakes at hub height that can be tracked from tens to over 100 kilometers downstream. Thus, wind turbines can reshape the wind profile and alter surface stresses and heat fluxes, which in turn can enhance or reduce surface mixing. The wind stress is the mechanical input of the wind's momentum into the water column, generating currents and turbulence. Heat fluxes refer to the heat lost or gained by the surface ocean layer, promoting stratification in case of warming, and overturning in case of cooling (Simpson & Sharples, 2012). Evaluating the potential effect of offshore wind turbines on surface and water column mixing in the MAB is the main motivation of this work, especially the evaluation of the mixing time scale when turbines are present and how they compare to the seasonal time scale. This allows a better understanding of nutrient cycling, light availability, and regional ecology with fully operating wind farms.

1.2 Project Objectives

The New Jersey Offshore Wind Research and Monitoring Initiative (RMI) has identified several high-priority research needs during the preconstruction phase of offshore wind development. The present study aligns with RMI research priorities: *the examination of offshore wind energy development on seafloor, light conditions, and ocean stratification (i.e., how could potential changes in circulation patterns due to offshore wind development affect geological and physical ocean properties, such as the Mid-Atlantic Cold Pool)*.

By investigating how offshore wind farms can affect ocean mixing, surface stress, and air-sea fluxes in the MAB, this study supports RMI's focus on changes in circulation patterns and ocean stratification, including the dynamics of the Cold Pool. This study comprises two tasks detailed below: one determines the time scales of mixing induced by offshore wind farm foundations such as monopiles, and the other investigates the potential impact of turbine wind wakes on the surface.

Task 1: Time Scales of Mixing and Offshore Wind Farms

This task is focused on ocean processes and wind turbine foundations, specifically as foundations obstruct ocean currents and produce turbulence that can accelerate mixing in a stratified water column. In the MAB, the water column overturns seasonally without wind turbines, with stratification increasing in spring, peaking in summer, and vanishing in fall, giving a seasonal or "natural" mixing time scale of 2-3 months. This task focuses on estimating whether wind turbines can accelerate mixing in the MAB over time scales comparable to the seasonal, using typical stratification and surface current values of the region as reference. The research question for this task is:

- *What is the potential role of monopile arrays on ocean mixing in the MAB due to the range of ocean processes that could induce mixing, such as daily tides or infrequent but strong storm events (e.g., hurricanes and Nor'easters)?*

Task 2: Impact of Offshore Wind Wakes on Stratification

Turbines at hub height harness energy from the wind field, creating velocity deficits and turbulent wakes that can affect momentum and heat fluxes at the ocean surface, which are critical for surface mixing. The research question for this task is:

- *What is the impact of turbine wind wakes on stress at the sea surface and the potential for increasing or reducing ocean mixing?*

In the next sections, we address each of these tasks separately and then present a unified discussion on monopile-induced (e.g., water column) and surface mixing.

2. Time Scales of Mixing and Offshore Wind Farms

This section contains the methodology (2.1), and results (2.2) of Task 1 related to obtaining the time scale of mixing due to OWFs in the region. The combined discussion for Tasks 1 and 2 is included in section 4.

2.1 Project Design and Methods

This task is based on idealized modeling of OWFs exposed to ocean currents, tailored to coastal ocean conditions in the MAB. The model, first applied in the North Sea by Carpenter et al. (2016), links the Turbulent Kinetic Energy (TKE) budget with a one-dimensional equation for stratification over time and depth. Here, TKE is the kinetic energy per unit mass associated with chaotic, small-scale eddies and swirls that vertically stir heat, nutrients, and momentum in the water column. In

this framework, monopiles are parameterized as rigid cylinders that generate turbulence when exposed to flow, eroding an initial stratification.

Goal:

The goal of this task is to estimate the time scales of mixing due to the interaction of currents and monopiles in the water relative to the seasonal time scale, which is in the order of ~3 months. Rather than seeking an exact mixing time, the time scale we seek is expressed as "order of" days, months, and years. Current computational constraints prevent high-resolution Large Eddy Simulations from being applied across wind-farm arrays—such models often focus on turbulence around a single monopile and do not scale regionally—while regional ocean models do not yet parameterize monopiles. Expressing mixing rates in orders-of-magnitude places turbine-driven mixing in the context of natural seasonal and interannual variability, providing regionally relevant insight into how offshore wind influences coastal stratification and transport without incurring prohibitive computational cost.

Model Assumptions:

- Vertical density gradients are more dynamically relevant than horizontal. Continental-shelf circulation and density variations typically span O(1–100 km) horizontally but only O(10 m) vertically. Because a gradient measures change over distance, the smaller vertical scale yields larger vertical gradients. This disparity justifies neglecting horizontal gradients in our one-dimensional vertical mixing model.
- Mixing is defined as the destruction of stratification. The only source of mixing in this model is the stirring (or shear production) produced by the monopile array. This allows focus on monopile-driven mixing rather than mixing due to air-sea fluxes and other sources.
- The model assumes a steady, depth averaged (i.e., vertically uniform) current, and a constant water depth. Tidal level variations in the MAB (order 0.5 m at the coast) are small relative to the depth of lease areas (~25 m). Some of the currents used in this study are typical of storm conditions, but we model them as a current and not the air-sea momentum flux that generated them. For surface fluxes, see section on Task 2.

Model output:

The model result is the mixing time scale due to monopiles (τ_{mix}). To ensure the consistency of the solution, this scale can be obtained in two modes:

- ***Steady:*** simplest way of approaching the problem with a constant pycnocline thickness. (The pycnocline thickness, where density changes rapidly with depth, extends from the base of the upper mixed layer to the top of the lower mixed layer).
- ***Unsteady:*** more detailed physics, considering a time-variable pycnocline thickness.

Model Physics and Mathematical Background:

The model considers an idealized density profile $\rho(z)$ for a stratified water column with upper and lower mixed layers and a pycnocline (i.e., a layer with a sharp density gradient). The total depth is H and the pycnocline thickness is b, as shown in Figure 2.

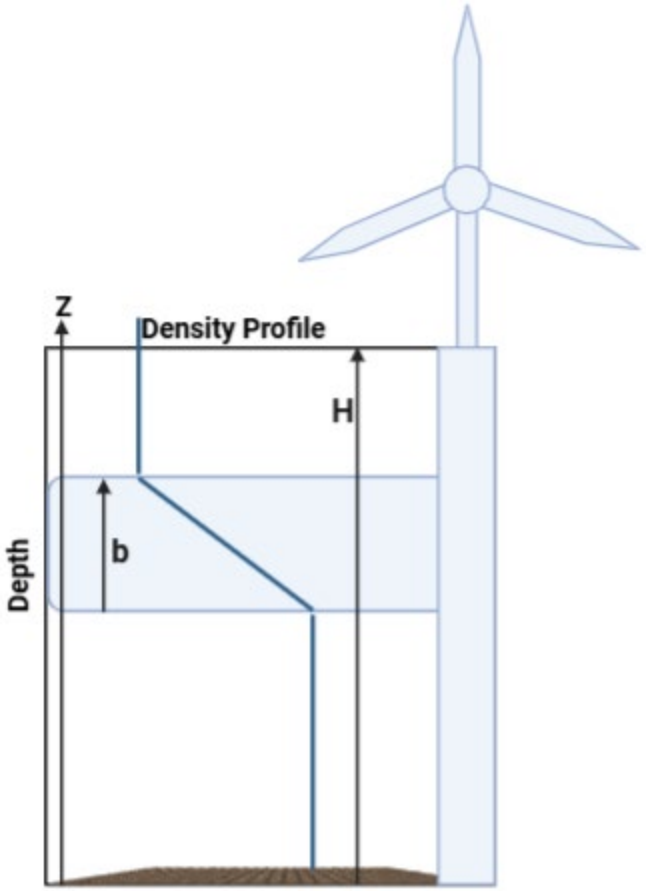

Figure 2. Idealized density profile (blue line) for a stratified water column. The total depth is H, the vertical coordinate (z) is positive upwards, and the pycnocline thickness is b. The pycnocline separates an upper mixed layer from the bottom layer (i.e., the Cold Pool).

To link stratification to a model of turbulent mixing, it is convenient to express it in terms of potential energy, or the gravitational energy stored in the column per unit area. A stratified water column is denser at the bottom and lighter on top, and its center of gravity is below mid-depth. A fully mixed water column has a constant density, and the center of gravity is at mid-depth. The potential energy anomaly (ϕ), a way to quantify stratification, is the energy required to overturn or mix the water column. Following Carpenter et al. (2016), the potential energy anomaly is:

$$\phi = \int_0^H [\rho_{mix} - \rho(z,t)]gz\,dz, \tag{1}$$

where g is the gravitational acceleration, ρ_{mix} is the density of the mixed water column, and $\rho(z,t)$ is the density as a function of depth and time. In this study, we use the above expression of ϕ with units J/m^2, though other authors express the potential energy anomaly as the depth average of (1); see e.g., Simpson et al. (1990); Simpson and Sharples (2012).

We are interested in how ϕ changes over time, therefore we take the time derivative of (1) to obtain:

$$\frac{d\phi}{dt} = -\int_0^H \frac{d\rho(z,t)}{dt} gz\, dz \tag{2}$$

The right-hand side of equation (2) contains a density tendency term ($d\rho/dt$). Based on the model assumption where density changes are only due to vertical mixing, we can express this process as turbulent diffusion,

$$\frac{d\rho}{dt} = \frac{d}{dz}\left(K\frac{d\rho}{dz}\right) \tag{3}$$

where K is the eddy viscosity. At this point, we introduce the TKE budget to link the eddy viscosity to mixing. In TKE terms, K is related to the buoyancy production (B) and the density profile,

$$B = K\frac{g}{\rho_0}\frac{\partial\rho}{\partial z} \tag{4}$$

Where ρ_0 is a reference density. Expressing K in terms of B, we can rewrite (3) as:

$$\frac{d\rho}{dt} = \frac{d}{dz}\left(\frac{\rho_0}{g}B\right) \tag{5}$$

Replacing (5) in (2), we obtain:

$$\frac{d\phi}{dt} = \rho_0\int_0^H \frac{dB}{dz} z\, dz \tag{6}$$

Using integration by parts,

$$\int_0^H \frac{\partial B}{\partial z} z\, dz = [zB]_0^H - \int_0^H B\ dz \tag{7}$$

Since the model assumes that turbulence is generated internally due to monopiles, we apply boundary conditions with no buoyancy fluxes at the vertical boundaries; $B(z=0)=0$ and $B(z=H)=0$. These conditions make the first term on the right-hand side zero, leaving:

$$\frac{d\phi}{dt} = \rho_0\int_0^H B\ dz \tag{8}$$

In this model, density changes are confined to the pycnocline (Figure 2), so the limits of the integral (8) become:

$$\frac{d\phi}{dt} = \rho_0\int_{h-\frac{b}{2}}^{h+\frac{b}{2}} B\ dz \tag{9}$$

Next, we consider that not all the turbulence generated by flow-monopile interactions can erode the stratification. This 'mixing inefficiency' is expressed by the flux Richardson number, R_f:

$$R_f = -\frac{B}{P} \tag{10}$$

where P is the shear production. A commonly reported value of R_f in the literature is 0.17. Using the flux Richardson number, we can rewrite (9) as:

$$\frac{d\phi}{dt} = -\rho_0 R_f \int_{h-\frac{b}{2}}^{h+\frac{b}{2}} P \, dz \tag{11}$$

Here, the shear production term explicitly represents the turbulence due to monopile-flow interactions. To express this term as a function of OWF dimensions and geometry, it needs to be idealized as an array of cylinders, with the number of cylinders per square kilometer representing a wind farm density. The cylinder properties, such as diameter and height, reflect typical manufacturer values for monopile or tripod foundations. Carpenter et al. (2016) found that the stirring (i.e., shear production) in W/m^2 due to flow passing through a cylinder array is given by:

$$P_{str} = \frac{\rho_0 C_D A u^3}{2l^2} \tag{12}$$

where C_D is the drag coefficient of the monopile, A is the area of the monopile facing the flow (i.e., the diameter times the depth), u is the depth-averaged ocean current speed, and l is the distance between monopiles, assuming a square grid configuration. This expression indicates that stirring is proportional to the drag coefficient and monopile frontal area, but particularly sensitive to the ocean current speed given the cube power, and to the squared distance between monopiles (l^2). Thus, the current speed has a disproportionate contribution to stirring.

According to theory, the drag coefficient has two contributions, one from skin drag related to the roughness of the monopile coating, plus any biofilms that develop on the surface, and another from pressure drag produced by flow separation. Skin drag is prevalent in low flow conditions rarely observed in the coastal ocean environment or at the spatial scales we are considering. Since coastal ocean flows are typically turbulent, it is reasonable to expect flow separation and pressure drag to constitute most of the drag. Carpenter et al. (2016) considered a drag coefficient interval of 0.6 – 1.0, which we will also adopt as 'low turbulence' and 'high turbulence' scenarios. The shear production term in W kg^{-1} is

$$P = \frac{P_{str}}{\rho_0 H} \tag{13}$$

Assuming that the shear production is uniform over depth, we get the final equation for the tendency of stratification:

$$\frac{d\phi}{dt} = -R_f P_{\mathrm{str}} \frac{b}{H} \tag{14}$$

Scaling $d\phi/dt$ in terms of an initial stratification and a time scale ($d\phi/dt \sim \phi/\tau_{mix}$), we find the **mixing time scale for the steady model**:

$$\tau_{\text{mix}} = \frac{\phi H}{R_f b P_{\text{str}}} \tag{15}$$

If we retain the time dependency of the pycnocline thickness, we obtain a **mixing time scale for the unsteady model**:

$$\tau_{\text{mix}} = \frac{g\Delta\rho H^2}{2\pi R_f P_{str}} \tag{16}$$

The model then reduces to expressions 15 (steady) and 16 (unsteady), requiring the following oceanographic and OWF inputs and parameters:

- Water Depth (H)
- Reference density (ρ_0)
- Current speed (u)
- Potential energy anomaly (ϕ, from density profile)
- Pycnocline thickness (b, from density profile)
- Monopile spacing (l)
- Drag coefficient (C_D)
- Monopile frontal area (A)

Application to the New Jersey Mid-Atlantic Bight

In this section, we describe the implementation of the mixing model to the MAB region. We design our model simulations to reflect conditions expected for the offshore wind lease areas closest to New Jersey, outlined in Figure 3. We use a reference depth for these lease areas of $H = 25$ m based on the approximate mean water depth of the lease areas.

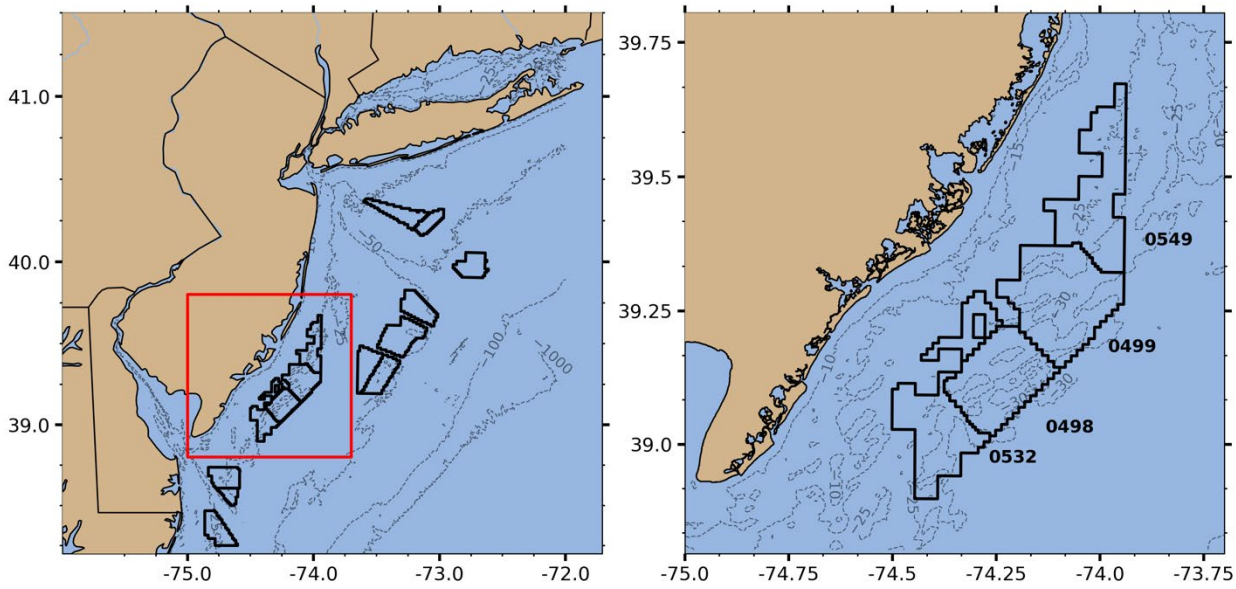

Figure 3. Study Region. (left) Broader New Jersey and neighboring states, and (right) zoom in to New Jersey Lease areas with identification codes.

Stratification: Stratification, in the form of potential energy anomaly, is a key input for the model. Here we follow Carpenter et al. (2016)'s approach where they use an idealized density profile informed by glider observations in the North Sea. While their study uses the maximum stratification from a single glider deployment as an input, we identify three representative periods in the MAB: *Setup* (May to June) with relatively low stratification and weak isolation of the bottom Cold Pool, *Peak* (July to August) with maximum stratification and a thick pycnocline, and *Breakdown* (September to October) with a deep surface mixed layer reflecting the transition into fall (Figures 4 and 5). We expect this approach to yield lower stratification values than the maximum value chosen in Carpenter et al. (2016), representing a conservative estimate of water column stratification. In our approach, to estimate the model input parameters for (16) and (17) and construct a profile similar to Figure 2, we identify the location of the Mixed Layer Depth (MLD) relative to the bottom, which are also the vertical limits that contain the pycnocline. Thus, the vertical limits of the pycnocline are defined as MLDL (L for 'lower') and MLDU (U for 'upper'), respectively, as shown in Figure 5. The pycnocline thickness (b in the model) is the difference between MLDU and MLDL.

To construct composite density profiles representative of the MAB, we retrieved Rutgers University glider data (https://slocum-data.marine.rutgers.edu/erddap/index.html) from 2010 to 2023 and selected glider tracks that entered the New Jersey lease areas coded 532, 498, 499, and 549 (Figure 4). We then divided the data into Setup, Peak, and Breakdown periods, each with 8038, 18457, and 23376 profiles, respectively.

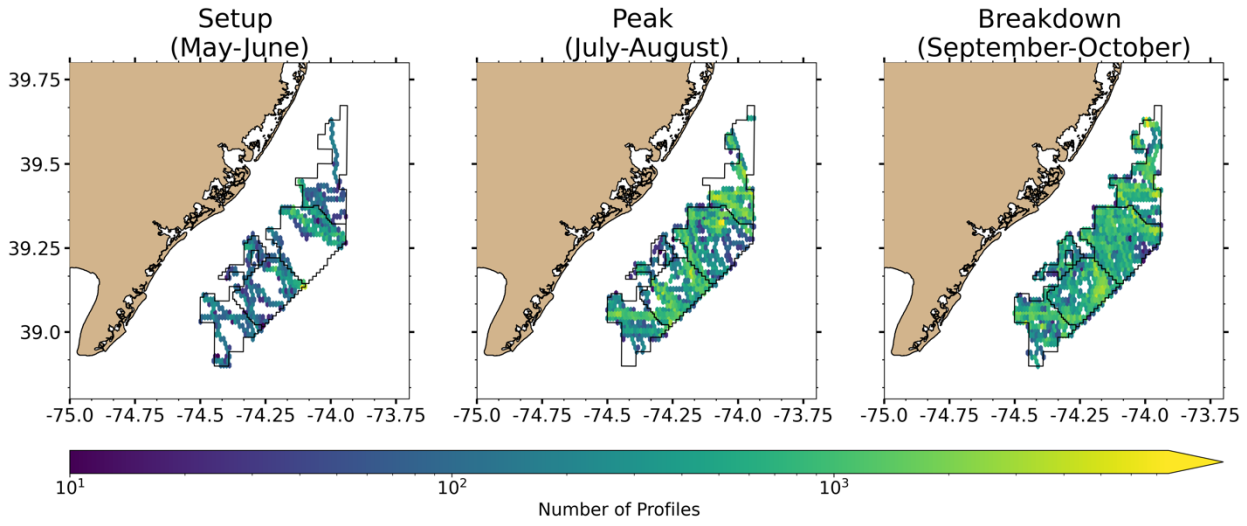

Figure 4. Glider profile counts and spatial coverage for the setup, peak, and breakdown periods.

We removed profiles where the shallowest depth exceeded 3 meters (e.g., where the glider did not sample in the surface layer), assuming these did not span the full water column. This filtering yielded 6369, 13406, and 15105 profiles for the respective periods. For each profile, we calculated the potential density, determined the MLDU and MLDL, following de Boyer Montégut et al. (2007), and computed the potential energy anomaly based on equation (1), following the Carpenter et al. (2016) study method. To reduce oversampling from gliders that collect hundreds of profiles per day, we took daily averages, which we then used to calculate the mean, median, and standard deviation for each variable (Table 1).

Table 1. Summary of Mixed Layer Depth (MLD) Upper and Lower datums and density values for setup, peak, and breakdown conditions, reported as mean ± standard deviation (median).

Condition	MLD Upper (m)	Density Upper (kg/m^3)	MLD Lower (m)	Density Lower (kg/m^3)
Set Up	8.86 ± 3.74 (7.79)	1024.08 ± 0.79 (1024.31)	15.47 ± 3.67 (14.44)	1025.20 ± 0.35 (1025.29)
Peak	8.58 ± 2.56 (8.44)	1021.03 ± 0.66 (1021.03)	17.17 ± 3.56 (17.45)	1024.09 ± 0.81 (1024.29)
Breakdown	15.30 ± 5.59 (15.26)	1022.15 ± 0.82 (1022.26)	18.88 ± 3.99 (18.74)	1023.22 ± 0.77 (1023.27)

Using values from Table 1, we assigned the mean density above the MLDU to the upper layer, and the mean density below the MLDL to the lower layer, then defined the pycnocline by linear interpolation between the two layers. We constructed the profile with a constant vertical resolution of 0.25-m. We generated profiles with depths extrapolated to 25-m. Where the 25-m depth represents the centroid depth of the lease area. The values of ϕ for the 25-m profiles during Setup, Peak, and Breakdown were 0.75 kJ/m^2, 2.22 kJ/m^2, and 0.66 kJ/m^2, respectively, with corresponding pycnocline thicknesses (b) of 6 m, 8 m, and 4 m. To align with the coordinate reference frame of the Carpenter et al. (2016) model, when constructing the composite density profile, we changed the reference frame to be 0 at the bottom, increasing to 25 at the surface. The MLDU and MLDL values in Figure 5, represent this new reference frame, while values of ϕ remain the same.

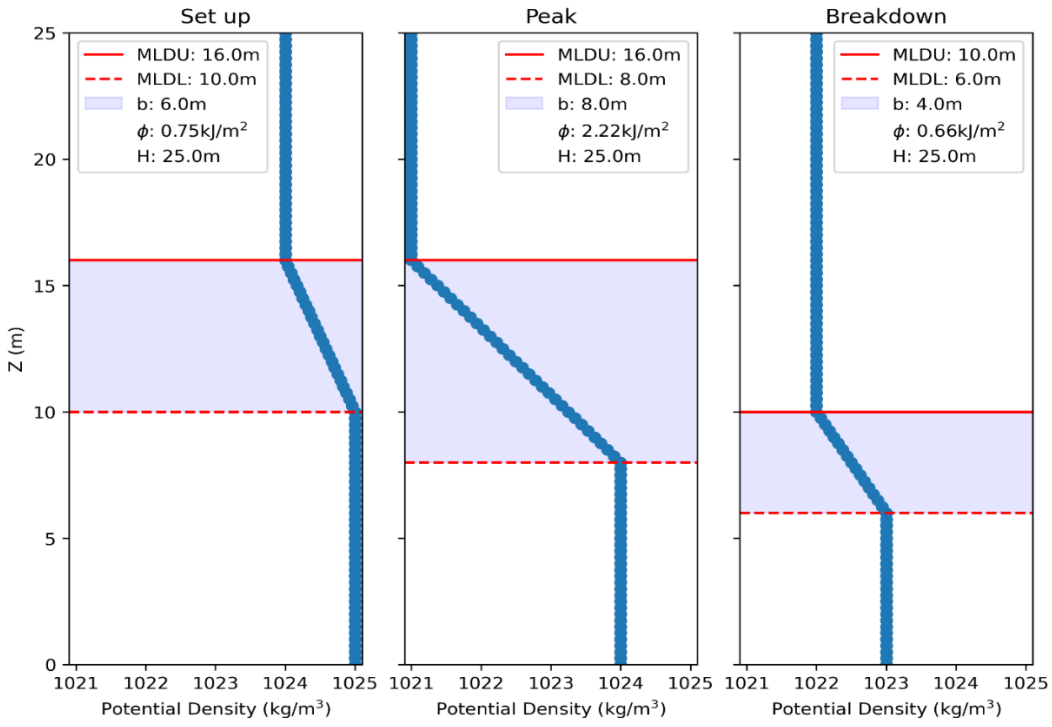

Figure 5. Initial composite potential density profiles for each season extrapolated to 25-m. The red solid line is the MLDU, the dashed red line is the MLDL, and the blue shaded region represents the pycnocline thickness, b. Here, z (upward positive) is the vertical coordinate (0 for the sea floor, 25 for the surface).

Currents and Drag: To select realistic current speeds for the model, we examined a 13-year (2010–2023) time series of depth-averaged currents from the Regional Ocean Modeling System (ROMS) DOPPIO model (López et al., 2020); see also https://tds.marine.rutgers.edu/erddap/info/index.html. DOPPIO covers the Mid-Atlantic Bight and Gulf of Maine regions on the US East Coast, operating on a 7-km spatial grid with 41 vertical layers to capture the complex coastal circulation in the region. We extracted hourly current magnitudes at 74.093° W and 39.273° N (i.e., the centroid of the OCS-0499 lease area), where we also composited glider data for the density profiles.

DOPPIO assimilates diverse data sources, including high frequency radar, glider observations, and satellite imagery, to generate a continuous estimate of the vertical ocean state for the full water column. Although regional model simulations do not capture every oceanographic process, they provide robust, order-of-magnitude estimates of currents that a single observing system cannot achieve. Figure 6 shows histograms of DOPPIO depth-averaged currents from 2010 to 2023 for the setup, peak, and breakdown periods.

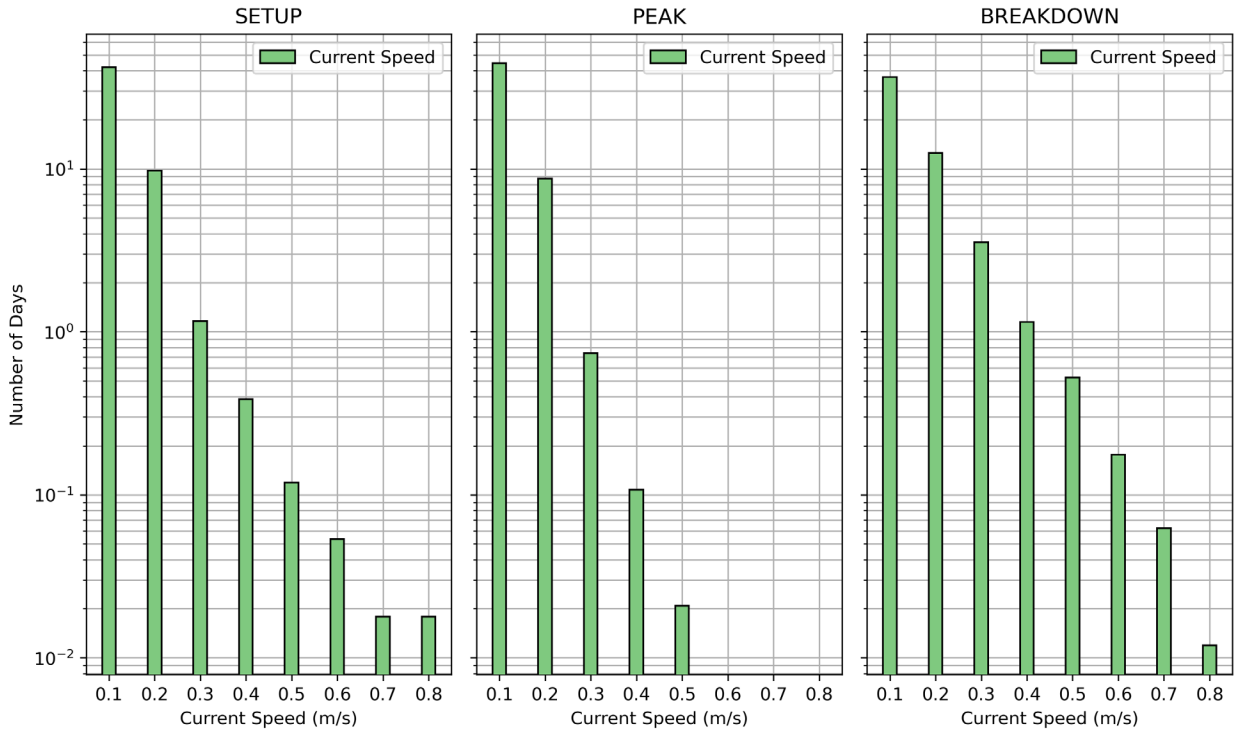

Figure 6. Histograms of DOPPIO current speeds at 74.093° W, 39.273° N (OCS-0499 centroid) for setup, peak, and breakdown from 2010 to 2023.

As shown in Figure 6, the most frequent current speed at the lease area centroid is about 0.1 m/s, corresponding to the semidiurnal lunar "M_2" tides. Current speeds above that value are less frequent and typically correspond to weather events such as cold fronts and nor'easters. The highest speeds over 0.7 m/s can be observed under tropical cyclones. Based on this information, we force the model with current speeds ranging from tidal (0.1 m/s) to storm-driven (0.8 m/s) in 0.01 m/s increments, and bin average the results into 0.1 m/s bins for visualization. Following Carpenter et al. (2016), we also consider runs with low ($C_D = 0.35$) and high ($C_D = 1.0$) turbulence to account for uncertainties in pressure drag.

Offshore Wind Farm Parameters: In the model, the spacing between monopiles is fixed at $l = 1$-km. This spacing is typical for projected wind farms in the region (Pareja-Roman et al., 2024), and consistent in order of magnitude (~10^3 m) with values from the Bureau of Ocean Energy Management (BOEM). The diameter of an individual monopile is 11.28-m, giving a frontal area $A = 282$-m^2 when H =25-m. These values follow a standard 15 MW turbine from NREL (National Renewable Energy Laboratory). The reference density of seawater, ρ_0, is 1023 kg/m^3.

Summary of Model Runs: We performed 960 model runs to assess the influence of stratification, current speed, and turbulence on mixing (Table 2). Three stratification scenarios were considered: Setup (0.75 kJ/m^2, b = 6-m), Peak (2.22 kJ/m^2, *b* = 8-m), and Breakdown (0.66 kJ/m^2, *b* = 4-m). For each scenario, the model was run with 80 different velocities (0.1 m/s to 0.8 m/s at 0.01 m/s increments), and two drag coefficients (0.35 for low and 1.0 for high turbulence), using both steady and unsteady approaches.

Table 2. Summary of model runs for the steady and unsteady models.

Input / Parameter	Value / Range
Stratification	Setup: 0.75 kJ/m^2, b = 6-m
	Peak: 2.22 kJ/m^2, b = 8-m;
	Breakdown: 0.66 kJ/m^2, b = 4-m
Currents	From 0.1 m/s to 0.8 m/s, 0.01 m/s increments into median Bins: 0.1, 0.2, 0.3, 0.4, 0.5, 0.6, 0.7, 0.8 m/s to align with DOPPIO model comparisons
Drag Coefficient	0.35 (low turbulence)
	1.0 (high turbulence)
Model type	Steady and Unsteady

2.2 Results

We present model experiment results in Figure 7 where we aggregate steady and unsteady model results for all 960 experiments into median bins along with reproduced velocities from the DOPPIO model (Figure 6). We present the steady model results for the Setup, Peak, and Breakdown periods, showing the mixing time scale in days for each velocity bin and turbulence scenario.

The analytical model simulations have output τ_{mix} described above, which is the time it would take the addition of turbines to fully mix the water column profiles presented in Figure 5. The DOPPIO current speeds are not necessarily consecutive but occur within each 2-month period. These analytical model results only represent mixing due to the addition of turbines, and do not account for other background de- or re-stratification processes that may occur between intermittent water column mixing events.

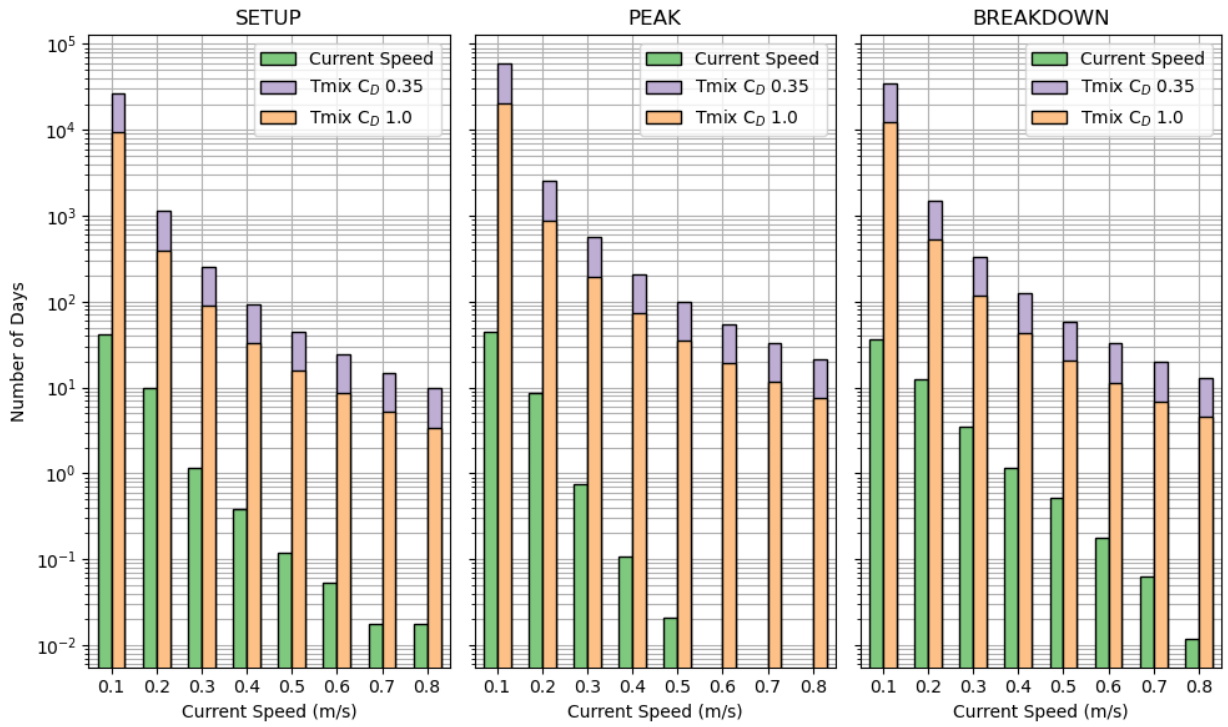

Figure 7. Time scales of mixing in days per median current speed bin (steady model) for the setup, peak, and breakdown periods. Green bars are histograms of DOPPIO current speed shown for reference. Orange and purple bars denote low and high turbulence (C_D) scenarios, respectively.

Results from the Steady State analytical model (Figure 7) show a mixing timescale of 10^4 days or approximately 27 years for current speeds of 0.1 m/s in both Setup and Breakdown seasons, and longer in the Peak stratification season. Current speeds in the 0.1 m/s increment are the most frequently occurring (~30 days of the 60-day long periods) and, based on these results, it is unlikely that turbines will lead to water column overturn. Generally, τ_{mix} values across all time periods and current speed increments are many orders of magnitude beyond the occurrence of DOPPIO simulated current speed increments. The closest τ_{mix} to the seasonal durations (Setup, Peak, and Breakdown periods are all 2 months) is 0.3 m/s (Setup), 0.4 m/s (Peak), and 0.3 m/s (Breakdown), which have values near 100 days. However, the corresponding velocity occurrences for those increments are on the order of 1 day. The shortest τ_{mix} times are ~10 days across all three seasons at 0.8 m/s, however current speed occurrences from DOPPIO at this speed only occur for a few hours in the Setup and Breakdown periods, and not at all in the Peak periods. τ_{mix} for the 'Unsteady' state model (Figure 8) are shorter, but the interpretation is generally consistent with the Steady State results. An integrated discussion of the findings can be found in Section 4.

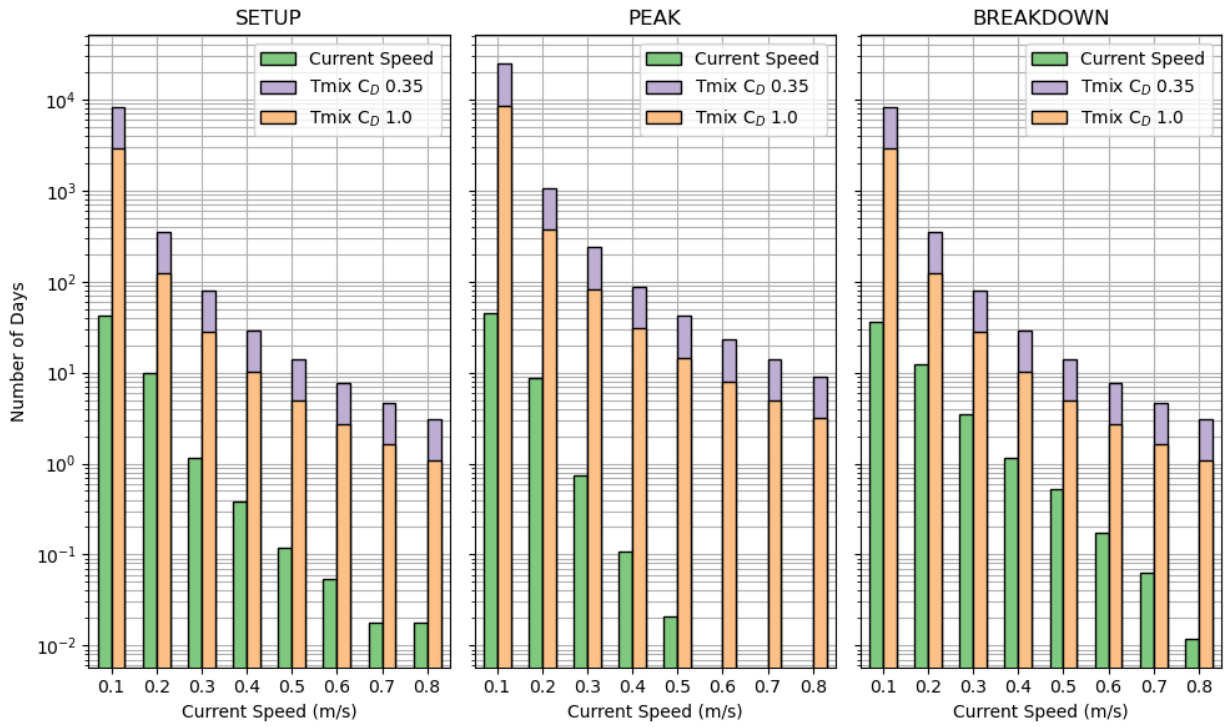

Figure 8. Time scales of mixing in days per median current speed bin (unsteady model) for the setup, peak, and breakdown periods. Green bars are histograms of DOPPIO current speed shown for reference. Orange and purple bars denote low and high turbulence (C_D) scenarios, respectively.

3. Wake Effects on the Surface

This section contains the methodology (3.1), and Results (3.2) of Task 2 related to the wake effects on the surface. Discussion is combined for the full study in section 4.

3.1 Project Design and Methods

The turbulent wake behind an offshore turbine can mix momentum, heat, and moisture throughout the marine boundary layer (see schematic in Figure 9). When wake-generated eddies penetrate downward, they can carry the low-momentum core to the sea surface (hereafter "surface"), reducing the 10 m wind speed and hence the surface stress that drives ocean mixing and generates currents. That surface stress is commonly expressed in terms of the friction velocity (i.e, a shear-based velocity scale whose square is proportional to the wind stress). At the same time, those turbulent motions can draw warmer or cooler, moister or drier air down into the lowest levels, altering the air temperature and the water-vapor mixing ratio (the mass of water vapor per unit mass of moist air). Together with the wind speed changes, these redistributions can modify the turbulent sensible heat flux (i.e., the upward turbulent transport of heat driven by the air–sea temperature difference), and the latent heat flux (the upward turbulent transport of moisture driven by the vertical humidity difference) (Hsu, 1988). By reshaping both momentum and buoyancy fluxes at the interface, turbine wakes may alter vertical mixing in the surface ocean. In this study we track how wakes influence five key variables: 10 m wind speed, 2 m air temperature, water-

vapor mixing ratio, friction velocity, and sensible heat flux—to assess their potential impact on ocean-surface mixing processes. The reference heights are relative to the sea surface.

In the MAB, a recent study by Golbazi et al. (2022) investigated the surface impacts of offshore wind farms, including New Jersey, New York, and Massachusetts wind lease areas. They employed the Weather Research and Forecasting (WRF) model with the Fitch et al. (2012) wind farm parameterization to compare scenarios with and without "extreme-scale" turbines (i.e., exceeding 150-m in rotor diameter, 100-m in hub height, and 10 MW in rated power). Their goal was to determine whether these larger turbines, which will likely dominate future offshore wind development, produce significant changes in surface meteorological variables such as temperature, wind speed, and turbulent air-sea fluxes.

Key findings by Golbazi et al. (2022) indicate that wind speed, turbulence, friction velocity, and sensible heat fluxes at the surface decrease only slightly with extreme-scale turbines, similar to conventional turbines. However, while conventional turbines can produce warming at the surface under stable atmospheric conditions, the warming from extreme-scale turbines remains confined below the rotor and does not extend to the surface, where minimal cooling was observed. Golbazi et al. (2022) concluded that, although the modeled changes in surface meteorological conditions are statistically significant, they remain negligible.

The Rutgers University Weather Research and Forecasting model, RUWRF (Optis et al., 2020) also covers the MAB and features wind turbines through the Fitch parameterization. While both the Golbazi et al. (2022) study and RUWRF are based on the WRF kernel, the model inputs and wind farm parameters are not identical. The goal of this task is to evaluate the impact of turbine wind wakes on the surface stress at the sea surface and the potential for increasing or reducing ocean mixing. In the next section we describe RUWRF, and the model used by Golbazi et al. (2022), identifying the differences that could potentially affect surface variables and fluxes.

Model Setup: Below is a comparative summary of the RUWRF and Golbazi et al. (2022) model setups (see also Table 3). RUWRF operates from 2019 to 2023, while Golbazi et al. (2022) conducted their simulations from June 1 to September 1, 2018. RUWRF relies on the Global Forecasting System (GFS) at 0.25° (~25 km) resolution for initial conditions, with six-hourly boundary updates, and employs the GOES-16 Spike-Filtered Sea Surface Temperature (SST) dataset (with daily imagery and a skin SST correction). In contrast, Golbazi et al. (2022) use the North American Mesoscale Forecast System (NAM) with a 12-km resolution for both initial and boundary conditions, updating every six hours, and NASA-JPL's daily SST data at 1-km resolution without a skin SST correction.

RUWRF runs with a base time step of 30 seconds and uses adaptive time stepping. Its domain configuration consists of three nested grids at 9-km, 3-km, and 1-km resolutions, centered on the New Jersey area. Golbazi et al. set a shorter base time step of 18 seconds and used a parent grid with a 4-km resolution along with two nested grids at 1.33-km resolution.

Table 3. Differences in WRF model setup for RUWRF and the Golbazi et al. (2022) models.

Parameter	RUWRF	Golbazi et al. 2022
Availability	2019–2023	June 1, 2018 – August 31, 2018
Initial Conditions	GFS at 0.25° resolution	NAM at 12-km resolution
Boundary Conditions	Updated every 6 hours from GFS	Updated every 6 hours from NAM
Sea Surface Temperature	GOES-16 Spike-Filtered Dataset (daily images)	NASA-JPL daily SST data at 1-km resolution
Time Step	30 seconds with adaptive stepping	18 seconds
Domains	Three nested grids: 9-km, 3-km, and 1-km; centered on the New Jersey area	One parent grid at 4-km with two nested grids at 1.33-km resolution

This comparison highlights differences and similarities between the two model setups, emphasizing how variations in initial/boundary conditions, SST data, temporal resolution, and grid configuration may affect simulations of offshore wind wakes and surface fluxes.

Model Physics: WRF physics schemes compute radiative, cloud, and turbulent processes. The cumulus (cu_physics) and microphysics (mp_physics) schemes simulate cloud processes, including formation and precipitation. The radiation schemes—shortwave (ra_sw_physics) and longwave (ra_lw_physics)—calculate energy exchanges by modeling how clouds, aerosols, and gases interact with radiation. The planetary boundary layer (bl_pbl_physics) scheme transports momentum, heat, and moisture, influencing turbulence at turbine heights. This turbulence, along with the fluxes computed by the surface scheme over water (sf_sfclay_physics), shapes the wind profile.

RUWRF and the Golbazi et al. (2022) models share the following schemes: Microphysics Option 8 (Thompson), Longwave Radiation Option 4 (Iacono), PBL Option 5 (Nakanishi & Niino, or MYNN), and Land Surface Physics Option 2 (Noah, Chen & Dudhia), while neither applies a cumulus parameterization. For shortwave radiation, RUWRF uses Goddard Option 5 (Chou & Suarez), whereas Golbazi et al. employ Option 4 (Iacono). Details of these schemes are available in the WRF manual: https://www2.mmm.ucar.edu/wrf/users/docs/user_guide_v4/v4.3/users_guide_chap5.html#Phys

The surface schemes over water (sf_sfclay_physics) used by RUWRF and Golbazi et al. differ, leading to variations in how the surface roughness and wind stress are computed. RUWRF employs Option 5, which uses the Mellor–Yamada–Nakaniishi–Niino (MYNN) scheme (Nakanishi & Niino, 2009). In this scheme, the surface roughness length follows the COARE 3.0 algorithm (Fairall et al., 2003), causing the roughness length to increase with wind speed up to approximately 19 m/s, and thus, making the wind stress more sensitive to wind speed. In contrast, Golbazi et al. (2022) use Option 2 based on the Monin–Obukhov with Janjić Eta scheme (Janjić, 1994), which produces a roughness length that is less responsive to wind speed. Despite these differences, discrepancies in surface roughness do not typically lead to large differences in ocean surface mixing, particularly within the typical wind speed ranges normally seen in the study region.

Wind Turbine Parameterization: The parameterization of wind turbines in WRF slightly differs between RUWRF and the Golbazi et al. (2022) study. Each model incorporates turbines using the Fitch et al. (2012) parameterization, but they vary in turbine spacing and specifications. For RUWRF,

the turbine integration focuses on wind lease areas in the Mid-Atlantic Bight and is applied only within the high-resolution 1-km nested domain. Key characteristics include:

- Turbines are spaced at 2-km intervals (every other grid cell).
- Each turbine has a hub height of 160-m.
- The rotor diameter is 200-m.
- Turbines follow NREL-15 MW specifications.

In contrast, Golbazi et al. (2022) employ one turbine per grid cell by spacing turbines at 8 to 10 times their diameter. Their study considers a range of turbine types referred to as Extreme Scale Turbines:

- DTU-10 MW: Hub height 119-m; rotor diameter 178-m.
- NREL-15 MW: Hub height 150-m; rotor diameter 240-m.

And conventional scale turbines*:*

- Gamesa-G128: Rated at 4.5 MW; hub height 81-m; rotor diameter 128-m.

Turbine hub height can influence how wind wakes affect the ocean surface. Lower turbines with larger rotor diameters are more likely to impact surface wind conditions. In this context, the NREL-15 MW turbine from Golbazi et al. (hub height 150-m, rotor diameter 240-m) is closest in dimensions to the RUWRF turbines, making it the most comparable for assessing wake effects at the surface.

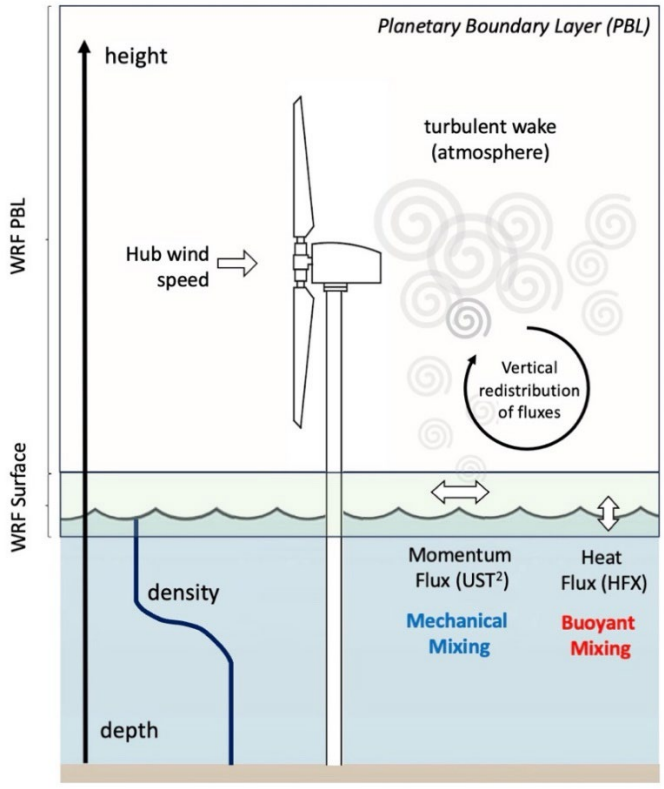

Figure 9. Schematic of Surface and Planetary Boundary Layer (PBL) Physics associated with wind wake effects at the ocean surface.

3.2 Results

Next, we show RUWRF model results of variables including wind speed at 10-m, air temperature and specific humidity at 2-m, surface friction velocity, and sensible heat flux to assess the impact of wind turbines and wakes and compare to the Golbazi et al. (2022) results. The model runs are labeled as "wind farm" and "control" (i.e., no wind farm parameterization) over the summer (June to August) 2022 period, where the RUWRF leveraged wind farm simulations were available. Below, we present the difference plots of the simulations with wind farms, minus the control, to demonstrate the relative modeled effect on each variable of wind wakes. Wherever possible, we use colormaps and data ranges to be consistent with Golbazi et al. (2022) for ease of intercomparison.

The average expected effect of wakes and turbines on the surface wind speed is shown in Figure 10. Wind speed reductions at 10-m were broadly under 0.5 m/s, with the largest reductions near the nearshore and offshore NJ lease areas, largely contained within the lease areas themselves.

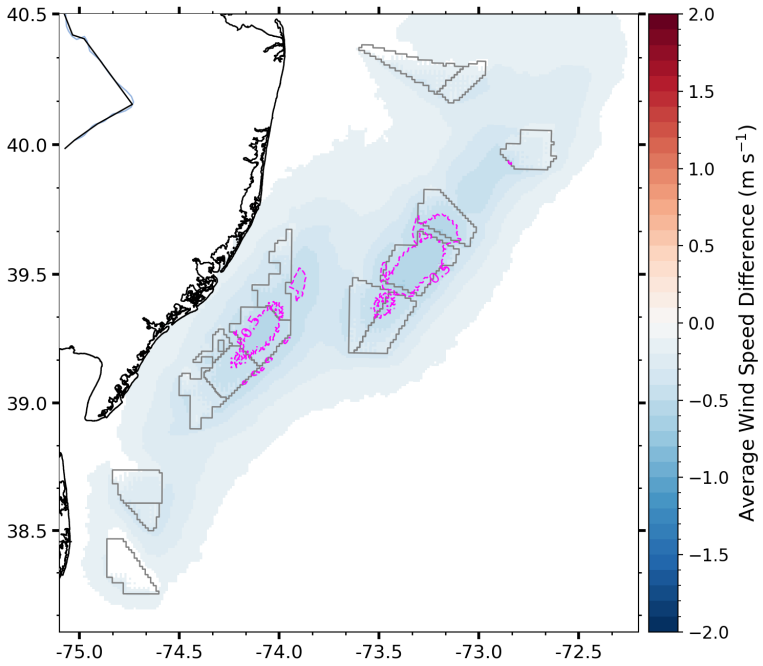

Figure 10. RUWRF model average wind speed difference at 10-m (wind farm – control) for summer 2022. The dashed lines are the -0.5 m/s wind speed difference.

RUWRF model air temperature differences (Figure 11) show warmer temperatures throughout the region of less than 0.05°C, with 0.1 to 0.05 °C within lease areas. There are cooler temperatures observed over coastal New Jersey; however, these values are approximately less than -0.01 °C and may be due to model noise. While RUWRF values were negative, those in Golbazi et al. 2022 were of similar magnitude but positive, potentially due to different satellite products as inputs, physics parameterizations, or different study periods. Regardless, the values in both studies are small and unlikely to impact water column stability meaningfully.

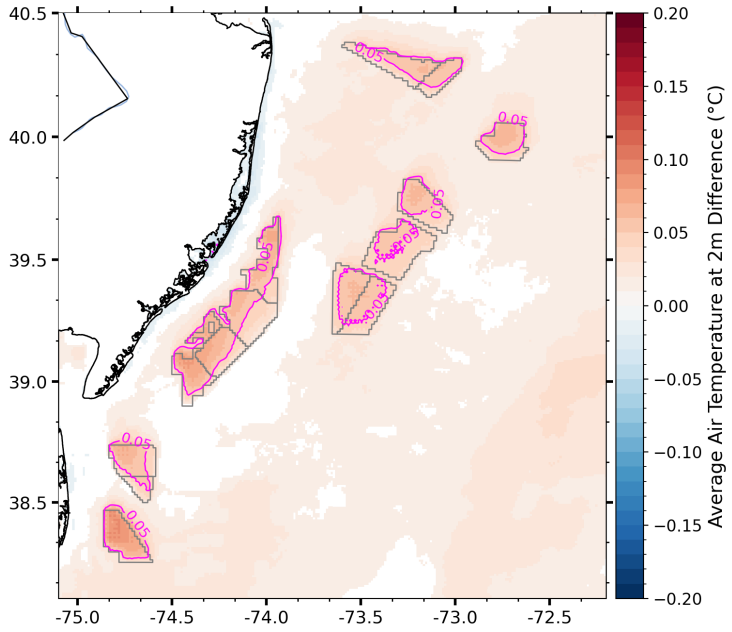

Figure 11. RUWRF model average air temperature difference at 2-m in °C (wind farm – control) for summer 2022. The dashed lines are the 0.05 °C temperature difference.

Figure 12 shows the average effect of wind turbines and wakes on the water vapor mixing ratio at the surface, a variable related to evaporation and latent heat fluxes. The presence of wind turbines leads to slightly drier air conditions, also as observed by Golbazi et al. (2022) who reported changes under 1% when turbines are present. Since the near surface humidity essentially acts as a minor correction to the surface buoyancy flux, which is driven by the sensible heat flux, we do not anticipate departures in humidity to affect surface ocean mixing.

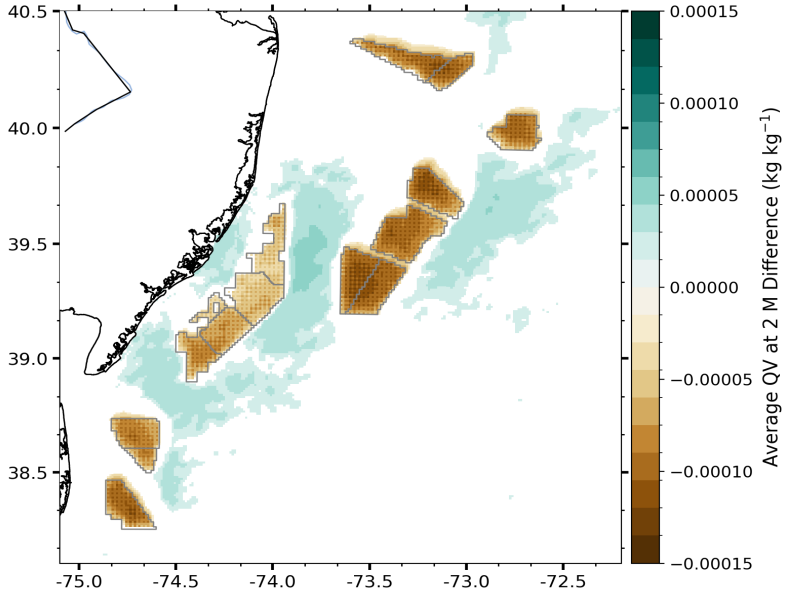

Figure 12. Difference (wind farm – control) in RUWRF model average water vapor mixing ratio (QV) at the surface for summer 2022.

Friction velocity differences (Figure 13) in RUWRF with and without turbines are also relatively small (~0.02 m/s), consistent with Golbazi et al. (2022), with both models indicating a slight reduction at the surface. When compared with the average magnitude of the friction velocity, this represents 10% of the total magnitude and is restricted to the interior of the wind lease areas.

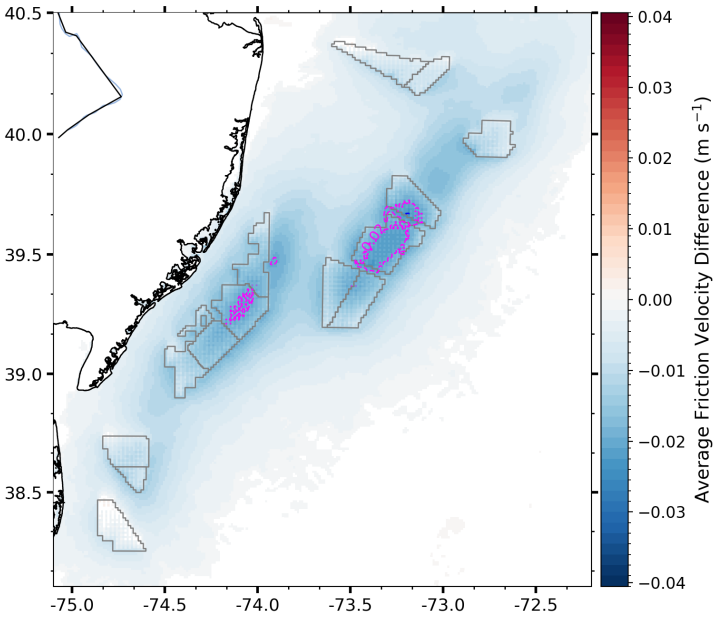

Figure 13. Difference (wind farm – control) in RUWRF average friction velocity at the surface for summer 2022. The dashed lines are the -0.02 m/s friction velocity difference.

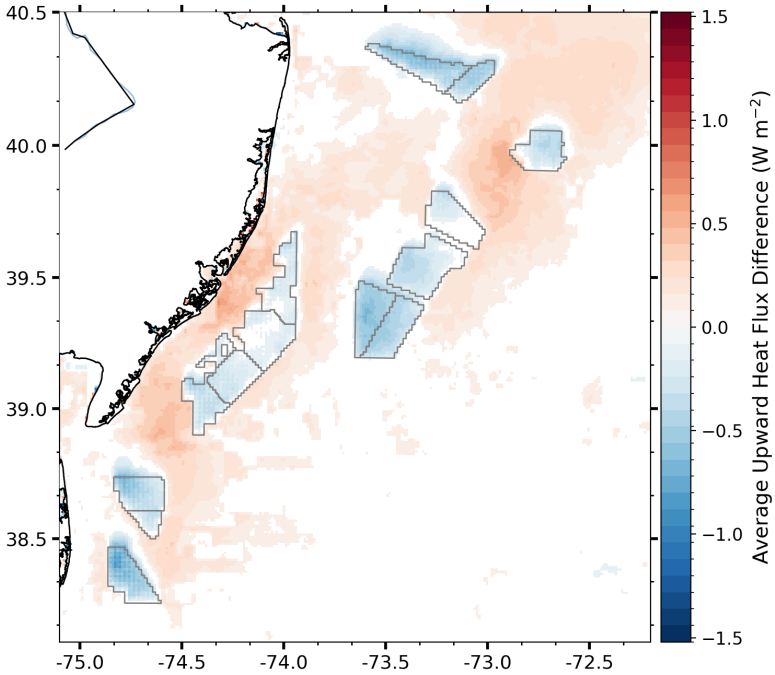

Figure 14. Difference (wind farm – control) in RUWRF average upward sensible heat flux at the surface for summer 2022.

Regarding the sensible heat flux at the sea surface (Figure 14), Golbazi et al. (2022) show that wind farms lead to slight warming (0.4 W/m^2) within lease areas, while RUWRF indicates slight cooling in and warming external to the lease areas. The differences between our study and Golbazi et al. (2022) again may be due to surface air-sea heat exchange parameterizations, different sea surface temperature products, and different study periods. However, the similarly small values of change lead us to believe that our simulations generally confirm the findings of Golbazi et al. (2022).

4. Discussion

Here, we combine the interpretation of our findings for both Task 1 and 2 studies. For Task 1, our analytical model simulations adapted from Carpenter et al. (2016) evaluated the time scale of mixing dependent on varying water column stratification and water velocity in the presence of turbine characteristics planned for the region. Overall, we find that the time required to fully mix the water column with turbines present—given the proposed turbine spacing, dimensions, background stratification, and current speeds ranging from 0.1 to 0.8 m/s—is at least one order of magnitude longer than the natural seasonal mixing timescale. .

While there are velocities in the region that could lead to water column overturn on time scales of a few days (>0.8 m/s), these speeds are only typically present for a few hours. These extreme current speeds are generally related to strong storm events, such as late- or early-season Nor'easters, or tropical storms, which are more common in the region during the breakdown season (Castelao et al., 2008). Velocities >0.8 m/s are not common in the region, but can occur. For example, glider observations in Superstorm Sandy in 2012 (Miles et al., 2017) measured velocities near 1 m/s for ~6 hours in the region offshore of our study site. However, they do not show up in the results here, as they occurred just after the breakdown study period.

Despite occasional extreme velocity events, typical long-term mean High-Frequency (HF) Radar surface currents have been documented to be between 0.02-0.12 m/s across the MAB (Roarty et al., 2020), and an area mean of 0.07 m/s within the Roarty et al. (2020) study region. Current speeds from that study showed increasing velocities toward the shelf-break, with weaker and more variable velocities in the nearshore zone. These velocities are similar to the depth averaged currents observed across the MAB in Lentz (2008) of ~0.05 m/s. Velocities when the ocean is stratified in spring, summer, and fall are typically weaker than those in the unstratified winter (Roarty et al., 2020); fall surface currents have the largest variability, which is likely due to the influence of fall transition storms, which overturn the water column and begin winter conditions. Despite seasonal variability, velocities extracted from ROMS, previous HF Radar surface current analyses (Roarty et al., 2020), and depth averaged currents (from in-situ moorings; Lentz, 2008) all indicate that velocities are typically on the order of 0.1 m/s, which correspond to extremely long (~27 years) turbine-induced water column turnover periods. These results suggest impacts to the Cold Pool from turbine foundations will be minor unless there are significant changes to water column stratification. We caution that the results of our analytical model are specifically focused on full water column turnover due to turbine foundations. While we don't expect turbines to have a significant impact on the setup or breakdown of the Cold Pool, this study does not address other potential impacts at smaller scales, such as increased turbulence due to wake foundations leading to nutrient injection during stratified conditions, or zooplankton patch dispersion (Saba, 2025).

Our Task 2 study focused on comparing the results of surface impacts from large wind farms between Golbazi et al. (2022) and similar model experiments using our RUWRF model. Our findings were generally consistent with theirs regardless of the different study periods and model physics choices detailed above. We confirm that the impact of turbine wakes on the sea surface are expected to be relatively minor and localized to the wind lease areas. For example, mean wind speeds decreased 0.5 m/s at the sea surface with turbines present, however, the effect was localized to the wind lease areas, and outside those regions, mean wind speed was reduced by less than 0.5 m/s (Figure 9). The impacts of wind speed reductions on the underlying water column are summarized in Miles et al. (2021): 1) a reduction in surface wind stress may lead to reduced upper ocean turbulence and mixing, resulting in a stabilizing effect on the water column (Afsharian & Taylor, 2019); and 2) reduced wind speeds may lead convergence and divergence of surface currents and drive localized upwelling dipoles (Broström, 2008; Paskyabi & Fer, 2012). The surface wind speed reductions assumed in Afsharian and Taylor (2019) were ~25%, well above the 5-10% (Figure 15) found in our simulations, while Broström (2008) assumed even larger reductions of ~30% to generate their upwelling-downwelling dipoles. Similar to Golbazi et al. (2022), we assume that the overall impacts on water column turbulence and mixing will be small for the proposed wind turbines here.

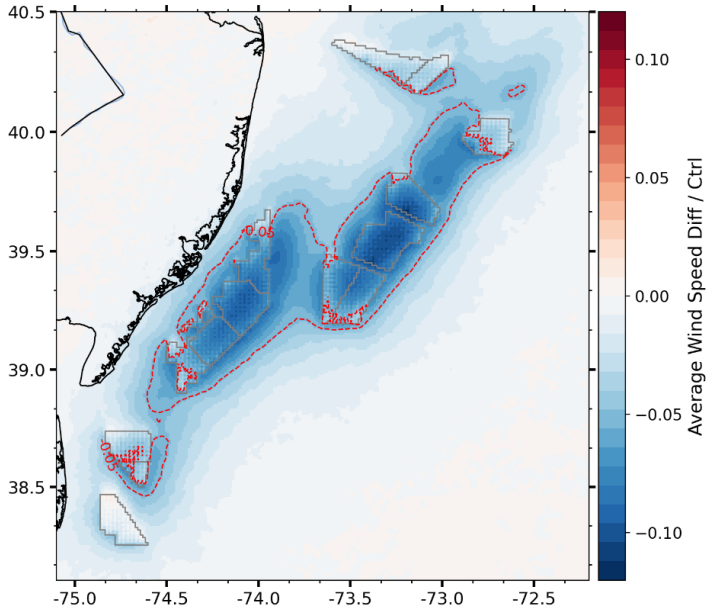

Figure 15. RUWRF model reduction in wind speed at 10 m height (wind farm relative to control)

Our simulations for Task 1 and interpretation of Task 2 assume that the Cold Pool stratification will remain constant, or not be reduced over the coming decades due to climate change. However, global climate models have predicted that the continental shelf of the Northeast US will have a warming trend (Saba et al., 2016). An analysis by Wallace et al. (2018) observed warming rates of ~0.5°C per decade over four decades largely due to atmospheric warming, while Forsyth et al. (2015) found 0.25°C per decade of warming, and Mountain (2003) found that 1990's MAB shelf waters were ~1°C warmer than the previous decade. A more recent study (Friedland et al., 2022) has found that the Cold Pool has warmed and reduced in size from 1968 – 2018 with a distinct shift in 2008. The strength of water column stability, which is proportional to the vertical density gradient in the region, is highly dependent on the rate of warming in the sea surface and bottom temperatures. For example, if the sea surface temperatures warm more rapidly than bottom temperatures, water column stratification and stability will increase. If the sea surface temperatures warm at the same rate as bottom

temperatures stability will remain constant. If the bottom temperatures (Cold Pool) warms faster than surface waters, stratification and stability will decrease. These rates are not well observed or resolved by regional or global climate models and require additional study to further interpret potential wind turbine impacts relative to climate scenarios.

5. Conclusions and Recommendations

Task 1 Conclusions:

- Based on our analytical model simulations, if turbines were installed in the proposed configuration and under the region's typical summer stratification and tidal currents (~0.1 m/s), it would take approximately 27 years to fully overturn the water column.
- The results of our mixing model experiments show that the water-column overturning caused by currents flowing past turbines requires velocities that, according to the realistic regional ROMS model, only occur for approximately one day per season. Because our simulations indicate overturning after approximately 60 days at these velocities, the study location experiences suitable currents less than 2% of the time, making sustained water-column overturning unlikely. There may still be smaller amounts of mixing, enhanced nutrient injection, and horizontal and vertical flow disturbances due to turbines. Future studies should focus on higher current speed time-frames and "shoulder" seasons when stratification is weaker.

Task 2 Conclusions:

- In this study, we confirmed the results of Golbazi et al. (2022) with the RUWRF model despite differing turbine parametrization decisions, physics parameterizations, bottom boundary conditions, and modeled periods.
- With the RUWRF model, expected wind speed reductions at the sea surface from turbines are small (~0.5 m/s or between 5 – 10% of the average wind speeds) and localized to the wind farm areas.
- We confirmed friction velocity reductions (UST) would be small (0.02 m/s) and localized to wind farm areas.
- We confirmed surface (2 m) air temperature changes would be small (±0.05) relative to summer temperatures of ~20 - 30ºC, even with different hub heights and schemes.
- We agree with the conclusions of Golbazi et al. (2022) that "Overall, the surface meteorological impacts of large offshore wind farms equipped with extreme-scale turbines are statistically significant but negligible in magnitude."

Recommendations:

Based on our findings in Task 1, we find it unlikely that the addition of turbines would fully overturn the water column, especially in peak stratification conditions (i.e., summer). Future investigations with more detailed ocean mixing models or observations may want to focus on the timing of spring Cold Pool setup or fall breakdown, or carry out detailed studies of high ocean velocity storm events. While it is unlikely that turbine foundations will fully overturn the water column, there is still the potential to disrupt ecosystems through smaller impacts on water column turbulence, downstream biogeochemistry, and/or physical aggregation of prey for higher trophic levels as detailed in the National Academies study on the "Potential Hydrodynamic Impacts of Offshore Wind Energy on the

Nantucket Shoals Regional Ecology" https://nap.nationalacademies.org/catalog/27154/potential-hydrodynamic-impacts-of-offshore-wind-energy-on-nantucket-shoals-regional-ecology.

Based on our findings in Task 2 and from Golbazi et al. (2022), we do not expect turbine wakes to have a significant impact on water column stability or mixing, and we do not recommend additional numerical modeling studies at regional scales. Limited in-situ studies of atmospheric wind wakes over the ocean environment have been carried out globally; therefore, it would be warranted to carry out observational studies and conduct more detailed wake simulations than those parameterizations included in the WRF models used here and in Golbazi et al. (2022) based on (Fitch et al. (2012).

6. Data Storage and Accessibility

In this project, no new data was collected. However existing datasets were utilized in model simulations, and model results and datasets were generated. Below, we provide instructions for access to well documented code to reproduce our results and analyses. Specifically, we have version controlled our code through GitHub, which is a web-based platform that uses Git, a version control system, that allows us to store, manage, and share code.

6.1 Task 1 Data Storage and Accessibility

Each component of the analysis has been coded into the Python computing language and continues to be hosted on the Rutgers University Center for Ocean Observing Leadership GitHub repository (https://github.com/rucool/rmi_hydrodynamics). The code referenced below can be identified in this repository.

Glider Data: Glider data was obtained from the Rutgers hosted and managed Environmental Research Division's Data Access Program (ERDDAP) server (https://slocum-data.marine.rutgers.edu/erddap/index.html), which also provides metadata for each deployment. The data can be accessed using the *glider2composite.ipynb* Python Jupyter notebook. This notebook utilizes ERDDAPY, a python module, to query the Rutgers ERDDAP server from 2010 to the present, clipping glider deployments to include only the portion of the tracks within the nearshore New Jersey Wind Lease Areas (WLAs) OCS-532, 498, 499, and 549.

Additionally, deployments were categorized into three periods: Cold Pool setup (May–June), peak (July–August), and breakdown (September–October). Mixed Layer Depth and Potential Energy Anomaly were calculated to generate composite profiles, which serve as inputs for the Carpenter mixing models (steady and unsteady state). The resulting *carp_pea_init_profs.csv* comma-separated values (CSV) file is stored in the *Glider_Data* folder within the GitHub repository. We store this data file as clipping the large volume of glider data takes a significant amount of computational resources and time to reproduce. This code is available for download only from the GitHub repository (https://github.com/rucool/rmi_hydrodynamics/blob/main/Glider_Data) as it retrieves a large amount of data and has a long runtime.

Carpenter Mixing 2016: The pair of Python Jupyter notebooks in the *carpenter_mixing_2016* folder within the GitHub repository implements the steady (*steady_state_model.ipynb)* and unsteady (*unsteady_model.ipynb)* state models as presented in Carpenter et al. (2016) and used in Cassin et al. (2024). Initialized using the *carp_pea_init_profs.csv,* these models estimate the time required for stratification to mix the water column across a range of current speeds as described above in the main text (0.1 to 0.8 m/s in 0.01 m/s increments), representing tidal and storm magnitudes. The steady and unsteady state model results are stored in the *carpenter_mixing_2016* folder within the GitHub repository as *steady_state_results_H25.csv* and *unsteady_results_H25.csv,* respectively. These files are relatively straightforward to reproduce with the code, which is available for download and to run using Google Colab, a cloud-based Jupyter Notebook environment executed in a browser, from the GitHub repository:
https://github.com/rucool/rmi_hydrodynamics/tree/main/carpenter_mixing_2016.

DOPPIO Depth Averaged Currents (DAC): Thirteen years (2010-2023) of hourly ROMS DOPPIO depth-averaged current velocities extracted at the centroid location of OCS-499 were obtained from the Rutgers Thematic Real-time Environmental Distributed Data Services (THREDDS) server (https://tds.marine.rutgers.edu/thredds/catalog/catalog.html). The server can be queried using the *DOPPIO_DAC.ipynb* Python Jupyter notebook. Additionally, this notebook uses the model results files (*steady_state_results_H25.csv* and *unsteady_results_H25.csv)* to compare mixing timescales to the extracted velocity data and generates a histogram. This code is available for download and to run using Google Colab, a cloud-based Jupyter Notebook environment executed in a browser, from the GitHub repository (https://github.com/rucool/rmi_hydrodynamics/tree/main/DOPPIO_DAC).

6.2 Task 2 Data Storage and Accessibility

Similar to Task 1 we provide access to the code used to perform data analysis and generate figures for Task 2 hosted through a GitHub repository:
https://github.com/rucool/wind-science/tree/master/rmi-ocean-mixing.

The RUWRF data used in this study was generated through a New Jersey Board of Public Utilities (NJBPU) research project and has been hosted at a THREDDS server for public access (https://tds.marine.rutgers.edu/thredds/catalog/cool/ruwrf/catalog.html). The code used to extract that data is detailed below, and instructions for its use are detailed in the GitHub repository above and reproduced below.

RUWRF Data extraction (wrf_data_wrangler_grid.py): pulls RUWRF output for a user-defined model domain/version and time range for a subset of variables and heights and saves each file to a user-defined directory. For this analysis, we pulled summer 2022 data monthly (June, July, August) from model domain/version 1km_ctrl (1km domain with no turbines) and 1km_wf2km_nyb (1km domain with a simulated windfarm including turbines spaced 2km apart and filling all wind energy lease areas in the New York Bight as of early 2023). This results in 3 Network Common Data Form (NetCDF) files (2022-06-01 to 2022-06-30, 2022-07-01 to 2022-07-31, and 2022-08-01 to 2022-08-31) for each variable. It's necessary to grab the data in small chunks because of the large volume of model output. Variables extracted and their units are described in detail in the NetCDF files, however a brief description follows: T2 (2m temperature), TEMP (temperature), U (wind speed in the east-west direction), V (wind speed in the north-south direction), U10 (as U for 10 m height), V10 (as V for 10m height), UST (surface friction velocity), Q2 (water vapor saturation ratio at 2 m), TKE_PBL (Turbulent

Kinetic Energy in the planetary boundary layer), HFX (air-sea sensible heat flux), TSK (surface skin temperature). Variables without a prescribed height were extracted at the surface, 120 m, 160 m, 200 m, and 300 m heights.

RUWRF Data averaging: (data_averages.py): This code generates averages of the datasets subset using wrf_data_wrangler_grid.py for a user-specified time range. For this analysis, we calculated averages for the entire summer 2022 (2022-06-01 to 2022-08-31). The runtime for this code can be quite significant, thus for convenience the resulting data files output from the scripts listed above are available at (https://marine.rutgers.edu/~lgarzio/rmi_ocean_mixing/) and can be used to generate the surface maps using the scripts below.

RUWRF Data Visualization (surface_maps_avgdiff.py): Generates surface maps for each variable at multiple heights (if applicable) from the files averaged using data_averages.py above. Maps include: Control model output (no simulated turbines), model output with simulated turbines, difference plots (turbines minus control), proportion reduction of turbines compared to the control (difference divided by control). We additionally supply the script (surface_map_tutorial.ipynb), which is a Jupyter notebook tutorial for generating surface maps from files containing summer 2022 average model output.

7. References

Afsharian, S., & Taylor, P. (2019). On the potential impact of Lake Erie wind farms on water temperatures and mixed-layer depths: Some preliminary 1-D modeling using COHERENS. *Journal of Geophysical Research: Oceans*, *124*(3), 1736-1749.

Broström, G. (2008). On the influence of large wind farms on the upper ocean circulation. *Journal of Marine Systems*, *74*(1-2), 585-591.

Carpenter, J. R., Merckelbach, L., Callies, U., Clark, S., Gaslikova, L., & Baschek, B. (2016). Potential Impacts of Offshore Wind Farms on North Sea Stratification. *Plos One*, *11*(8). https://doi.org/ARTN e016083010.1371/journal.pone.0160830

Cassin, R., Miles, T. N., & Pareja-Roman, L. F. (2024). Investigating Potential Impacts of Offshore Wind Turbine Foundations on the Mid-Atlantic Bight Cold Pool. 2024 Ocean Sciences Meeting,

Castelao, R., Glenn, S., Schofield, O., Chant, R., Wilkin, J., & Kohut, J. (2008). Seasonal evolution of hydrographic fields in the central Middle Atlantic Bight from glider observations. *Geophysical Research Letters*, *35*(3).

Fairall, C. W., Bradley, E. F., Hare, J. E., Grachev, A. A., & Edson, J. B. (2003). Bulk parameterization of air-sea fluxes: Updates and verification for the COARE algorithm. *Journal of Climate*, *16*(4), 571-591. https://doi.org/Doi 10.1175/1520-0442(2003)016<0571:Bpoasf>2.0.Co;2

Falkowski, P., Vidal, J., Hopkins, T., Rowe, G., Whitledge, T., & Harrison, W. (1983). Summer nutrient dynamics in the Middle Atlantic Bight: primary production and utilization of phytoplankton carbon. *Journal of Plankton Research*, *5*(4), 515-537.

Fitch, A. C., Olson, J. B., Lundquist, J. K., Dudhia, J., Gupta, A. K., Michalakes, J., & Barstad, I. (2012). Local and Mesoscale Impacts of Wind Farms as Parameterized in a Mesoscale NWP Model. *Monthly Weather Review*, *140*(9), 3017-3038. https://doi.org/https://doi.org/10.1175/MWR-D-11-00352.1

Flagg, C., Wirick, C., & Smith, S. L. (1994). The interaction of phytoplankton, zooplankton and currents from 15 months of continuous data in the Mid-Atlantic Bight. *Deep Sea Research Part II: Topical Studies in Oceanography*, *41*(2-3), 411-435.

Forsyth, J. S. T., Andres, M., & Gawarkiewicz, G. G. (2015). Recent accelerated warming of the continental shelf off New Jersey: Observations from the CMV O leander expendable bathythermograph line. *Journal of Geophysical Research: Oceans*, *120*(3), 2370-2384.

Friedland, K. D., Miles, T., Goode, A. G., Powell, E. N., & Brady, D. C. (2022). The Middle Atlantic Bight Cold Pool is warming and shrinking: indices from in situ autumn seafloor temperatures. *Fisheries Oceanography*, *31*(2), 217-223.

Golbazi, M., Archer, C. L., & Alessandrini, S. (2022). Surface impacts of large offshore wind farms. *Environmental Research Letters*, *17*(6), 064021. https://doi.org/10.1088/1748-9326/ac6e49

Haidvogel, D. B., Arango, H., Budgell, W. P., Cornuelle, B. D., Curchitser, E., Di Lorenzo, E., Fennel, K., Geyer, W. R., Hermann, A. J., Lanerolle, L., Levin, J., McWilliams, J. C., Miller, A. J., Moore, A. M., Powell, T. M., Shchepetkin, A. F., Sherwood, C. R., Signell, R. P., Warner, J. C., & Wilkin, J. (2008). Ocean forecasting in terrain-following coordinates: Formulation and skill assessment of the Regional Ocean Modeling System. *Journal of Computational Physics*, *227*(7), 3595-3624. https://doi.org/10.1016/j.jcp.2007.06.016

Houghton, R. W., Schlitz, R., Beardsley, R. C., Butman, B., & Chamberlin, J. L. (1982). The Middle Atlantic Bight cold pool: Evolution of the temperature structure during summer 1979. *Journal of Physical Oceanography,* 12(10), 1019-1029

Janjić, Z. I. (1994). The step-mountain eta coordinate model: Further developments of the convection, viscous sublayer, and turbulence closure schemes. *Monthly Weather Review*, *122*(5), 927-945.

Lentz, S. J. (2008). Observations and a model of the mean circulation over the Middle Atlantic Bight continental shelf. *Journal of Physical Oceanography*, *38*(6), 1203-1221.

Lentz, S. J. (2017). Seasonal warming of the Middle Atlantic Bight Cold Pool. *Journal of Geophysical Research: Oceans,* 122(2), 941-954.

López, A. G., Wilkin, J. L., & Levin, J. C. (2020). Doppio–a ROMS (v3. 6)-based circulation model for the Mid-Atlantic Bight and Gulf of Maine: configuration and comparison to integrated coastal observing network observations. *Geoscientific Model Development*, *13*(8), 3709-3729.

Miles, T., Murphy, S., Kohut, J., Borsetti, S., & Munroe, D. (2021). Offshore wind energy and the Mid-Atlantic Cold Pool: a review of potential interactions. *Marine Technology Society Journal*, *55*(4), 72-87.

Miles, T., Seroka, G., & Glenn, S. (2017). Coastal ocean circulation during Hurricane Sandy. *Journal of Geophysical Research: Oceans*, *122*(9), 7095-7114. https://doi.org/https://doi.org/10.1002/2017JC013031

Mountain, D. G. (2003). Variability in the properties of Shelf Water in the Middle Atlantic Bight, 1977–1999. *Journal of Geophysical Research: Oceans*, *108*(C1).

Nakanishi, M., & Niino, H. (2009). Development of an improved turbulence closure model for the atmospheric boundary layer. *Journal of the Meteorological Society of Japan. Ser. II*, *87*(5), 895-912.

Optis, M., Kumler, A., Scott, G., Debnath, M., & Moriarty, P. (2020). *Validation of RU-WRF, the Custom Atmospheric Mesoscale Model of the Rutgers Center for Ocean Observing Leadership*. . https://www.nrel.gov/docs/fy20osti/75209.pdf

Pareja-Roman, L. F., Miles, T., & Glenn, S. (2024). Coastal Upwelling Modulates Winds and Air-Sea Fluxes, Impacting Offshore Wind Energy. *Frontiers in Energy Research*, *12*. https://doi.org/10.3389/fenrg.2024.1470712

Paskyabi, M. B., & Fer, I. (2012). Upper ocean response to large wind farm effect in the presence of surface gravity waves. *Energy Procedia*, *24*, 245-254.

Roarty, H., Glenn, S., Brodie, J., Nazzaro, L., Smith, M., Handel, E., Kohut, J., Updyke, T., Atkinson, L., & Boicourt, W. (2020). Annual and seasonal surface circulation over the Mid-Atlantic Bight Continental Shelf derived from a decade of High Frequency Radar observations. *Journal of Geophysical Research: Oceans*, *125*(11), e2020JC016368.

Saba, G. K. (2025). Zooplankton and Offshore Wind: Drifters in a Sea of Uncertainty. *Oceanography*. https://doi.org/10.5670/oceanog.2025.302

Saba, V. S., Griffies, S. M., Anderson, W. G., Winton, M., Alexander, M. A., Delworth, T. L., Hare, J. A., Harrison, M. J., Rosati, A., & Vecchi, G. A. (2016). Enhanced warming of the Northwest Atlantic Ocean under climate change. *Journal of Geophysical Research: Oceans*, *121*(1), 118-132.

Secor, D. H., Zhang, F., O'Brien, M. H., & Li, M. (2019). Ocean destratification and fish evacuation caused by a Mid-Atlantic tropical storm. *Ices Journal of Marine Science*, *76*(2), 573-584.

Simpson, J. H., Brown, J., Matthews, J., & Allen, G. (1990). Tidal straining, density currents, and stirring in the control of estuarine stratification. *Estuaries*, *13*(2), 125-132. https://doi.org/10.2307/1351581

Simpson, J. H., & Sharples, J. (2012). *Introduction to the Physical and Biological Oceanography of Shelf Seas*. Cambridge University Press. https://books.google.com/books?id=kzggAwAAQBAJ

Skamarock, W. C., Klemp, J. B., Dudhia, J., Gill, D. O., Liu, Z., Berner, J., Wang, W., Powers, J., Duda, M., & Barker, D. (2019). A description of the advanced research WRF version 4. *NCAR tech. note ncar/tn-556+ str*, *145*.

Sower, J. R., Robillard, E., Powell, E. N., Hemeon, K. M., & Mann, R. (2022). Defining patterns in ocean quahog (Arctica islandica) sexual dimorphism along the Mid-Atlantic Bight. *Journal of Shellfish Research*, *41*(3), 335-348.

Wallace, E. J., Looney, L. B., & Gong, D. (2018). Multi-decadal trends and variability in temperature and salinity in the Mid-Atlantic Bight, Georges Bank, and Gulf of Maine. *Journal of Marine Research*, *76*, 163.

8. Appendices

8.1 List of Publications and Presentations

Presentations given on this project to date are:

- Pareja-Roman, L.F.; Miles, T.N. (2024*). An Investigation of Potential Impacts of Wind Turbine and Foundations on the Cold Pool*. 2nd Annual Research and Monitoring Initiative (RMI) Symposium. Monmouth University. New Jersey, United States.
- Miles, T.N., (2024). *Offshore Wind and the Mid-Atlantic Bight Cold Pool*. Seminar for the Center for Coastal Physical Oceanography (CCPO) and Institute for Coastal Adaptation and Resilience (ICAR). Old Dominion University. Norfolk, Virginia. United States.
- Miles, T.N., (2025) *An Investigation of Potential Impacts of Wind Turbine and Foundations on the Cold Pool*. 3rd Annual Research and Monitoring Initiative (RMI) Symposium. Stockton University – Atlantic City Campus. New Jersey, United States.